

Energetic Interpenetrating Polymer Network (EIPN): Enhanced Thermo-Mechanical Properties of NCO-*f*MWCNTs/HTPB PU and Alkyne-*f*MWCNTs/Acyl-GAP based Nanocomposite and its Propellants

(Supporting Information)

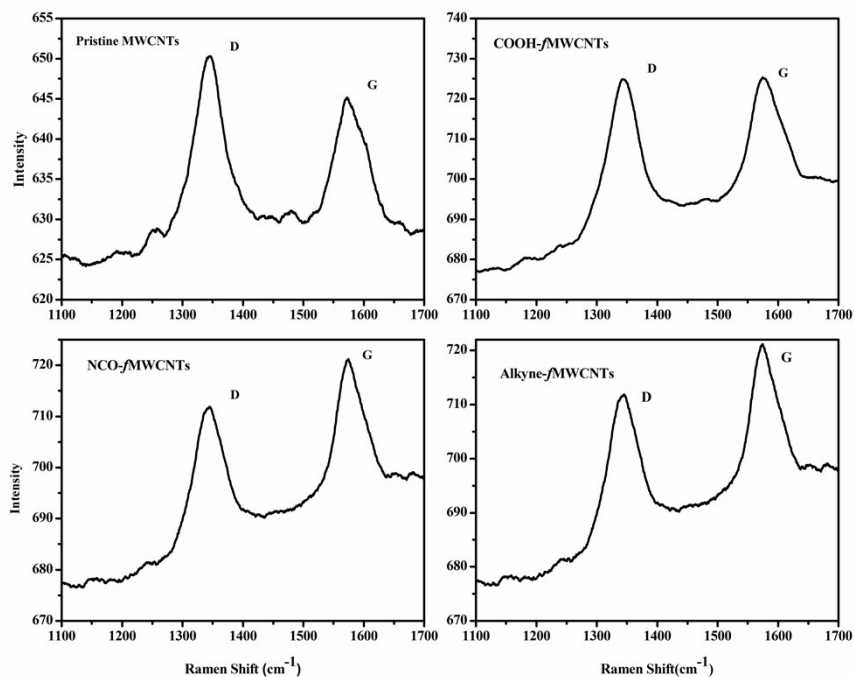


Figure 1: Raman spectra of pristine MWCNTs, COOH-*f*MWCNTs, NCO-*f*MWCNTs and Alkyne-*f*MWCNTs

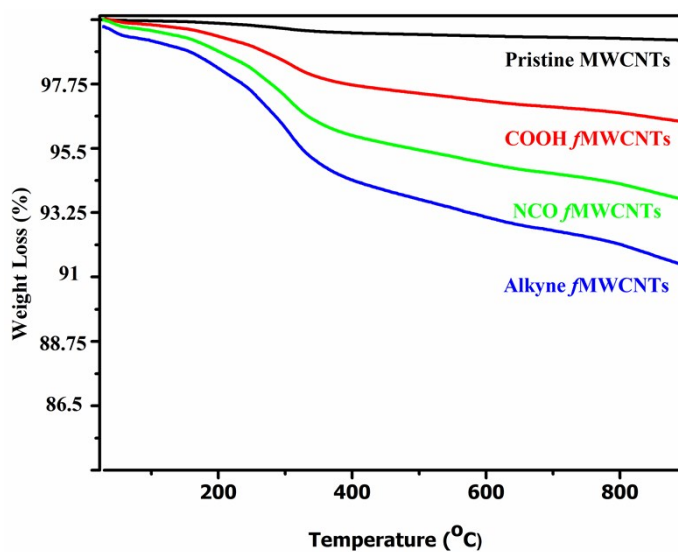


Figure 2: TGA curves of pristine MWCNTs, COOH-*f*MWCNTs, NCO-*f*MWCNTs and Alkyne-MWCNTs up to 900 °C.

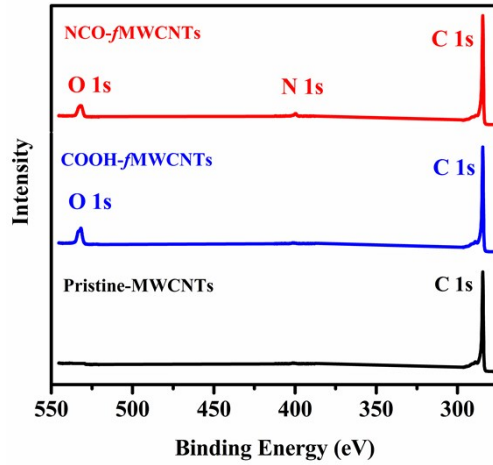


Figure 3: XPS survey scans of pristine MWCNTs, COOH-fMWCNTs and NCO-fMWCNTs.

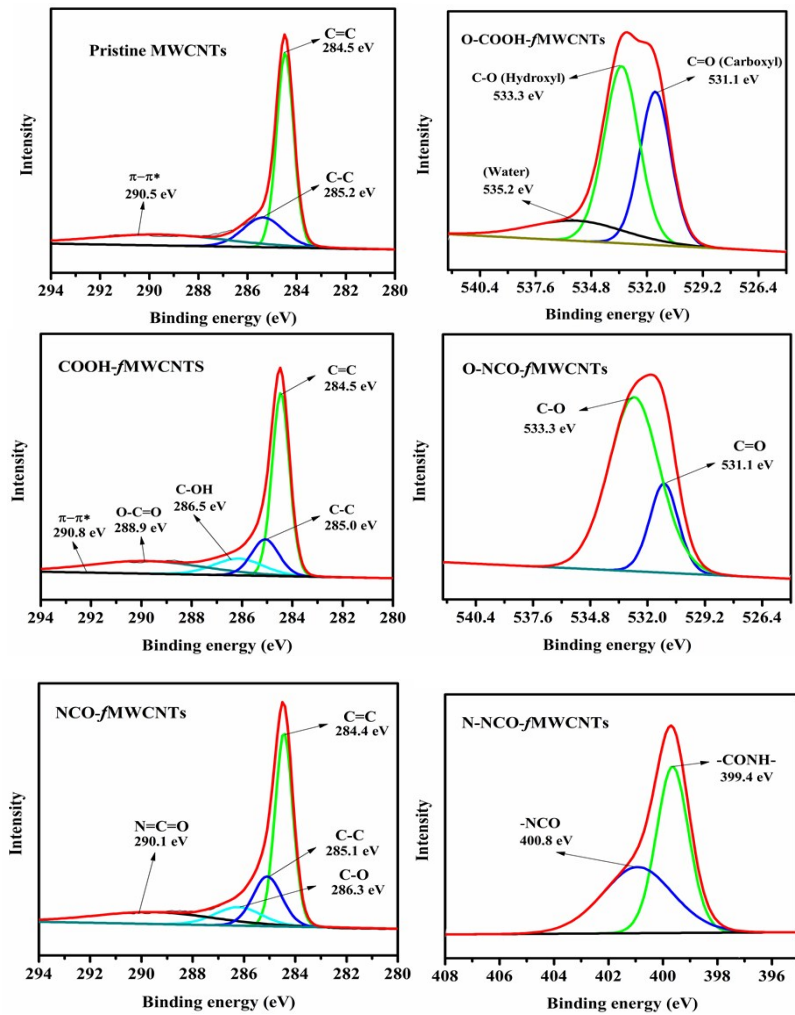


Figure 4: High resolution C1s XPS spectra of pristine MWCNTs, COOH-fMWCNTs and NCO-fMWCNT .

Figure 5: High resolution O1s and N1s XPS spectra of COOH-fMWCNTs

Table 1: Mechanical properties and thermal properties of various propellants cured with different curing agents

CONSTITUENTS	GAP/IPDI/N100 NCO/OH = 1 (Wt. %)	HTPB/IPDI/N100 NCO/OH = 1 (Wt. %)	Alkyne-fMWCNTs Acyl-GAP (Wt. %)	NCO-fMWCNTs/ HTPB NCO/OH=1 (Wt. %)	NCO-fMWCNTs HTPB / Alkyne-fMWCNTs Acyl-GAP (Wt. %)
Mech Prop. (21 °C)					
Tensile st. / MPa	0.37	0.62	0.59	0.86	0.97
Elong at Brek. (%)	25	47	41	58	63
Thermal Prop.					
Tg DMA 1 Hz	- 37.8	- 76.6	- 37.3	- 78.0	- 75.3 °C & - 36 °C
DSC onset °C	- 33.5	- 81.8	- 32.6	- 83.8	- 81.7 °C & - 38 °C
DSC offset °C	- 39.4	- 72.8	- 40.6	- 74.2	- 71.3 °C & - 36 °C
Mid-point °C	- 36.6	- 75.3	- 36.5	- 77.5	- 75.4 °C & - 36 °C

Table 2: Theoretical Ballistic properties of various propellants with 80 and 60 % Solid loadings

Ballistic Property	Alkyne fMWCNTs Acyl-GAP (Wt. %) (80 % Solid)	NCO-fMWCNTs/ HTPB NCO/OH=1 (Wt. %) (80 % Solid)	NCO-fMWCNTs HTPB / Alkyne-fMWCNTs Acyl-GAP (Wt. %) (80 % Solid)	ADN/GAP- BuNENA (80 % Solid)	HMX/GAP- BuNENA (80 % Solid)	HMX/GAP- BuNENA (60 % Solid)
Theoretical Specific Impulse I_{sp} (Ns kg ⁻¹)	2684.8	2621.6	2652.1	2601 (Ref :67)	2404 (Ref : 67)	2163 (Ref : 67) 2154 (Ref : 68)
Theoretical density (gcm ³)	1.85	1.767	1.80			
Oxygen balance (OB)	-0.554	-0.778	-0.685			
Density Impulse	4966.88	4632.36	4773.78			

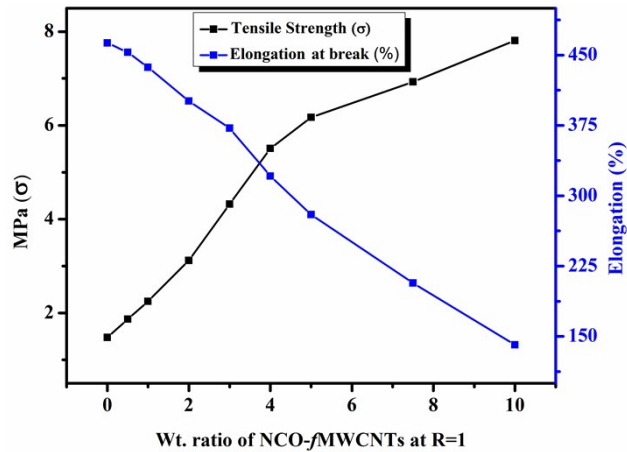


Figure 6: Effect of NCO-fMWCNTs on the tensile strength (σ) and breaking elongation (ϵ_b) of HTPB at R=1.

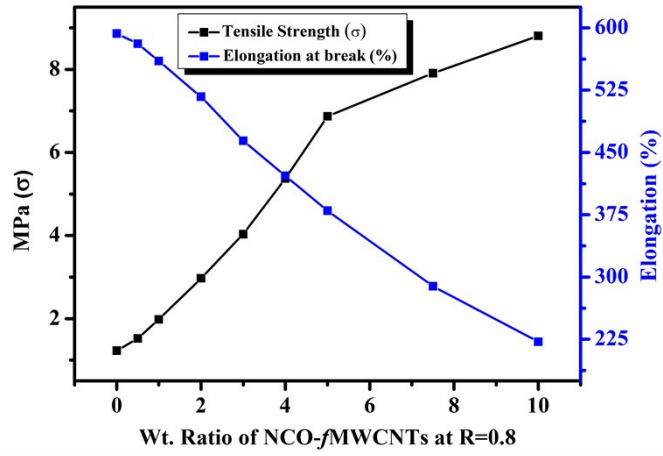


Figure 7: Effect of NCO-fMWCNTs on the tensile strength (σ) and breaking elongation (ϵ_b) of HTPB at R=0.8.

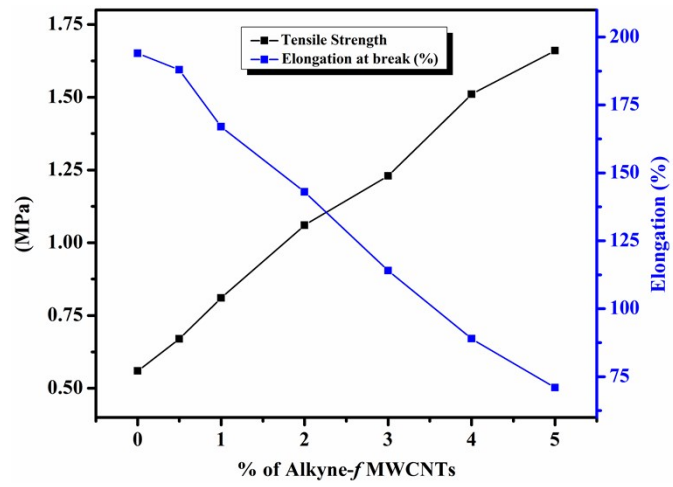


Figure 8: Effect of Alkyne-fMWCNTs on the tensile strength (σ) and breaking elongation (ϵ_b) of Acyl-GAP.

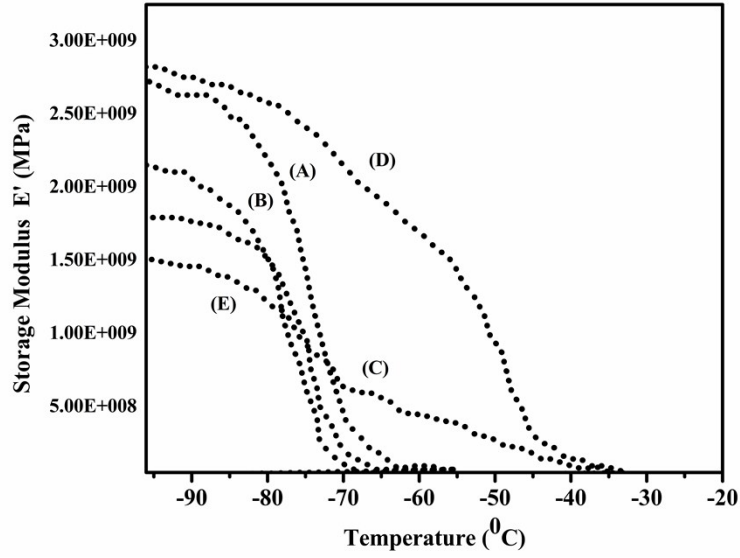


Figure 9. Variation of storage modulus with temperature for (A) 0 % Acyl-GAP, (B) 10 %, (C) 30 % (D) 50 %, (E) 70 % Acyl-GAP in NCO-*f*MWCNTs/HTPB: Alkyne-*f*MWCNTs/Acyl-GAP EIPNs.

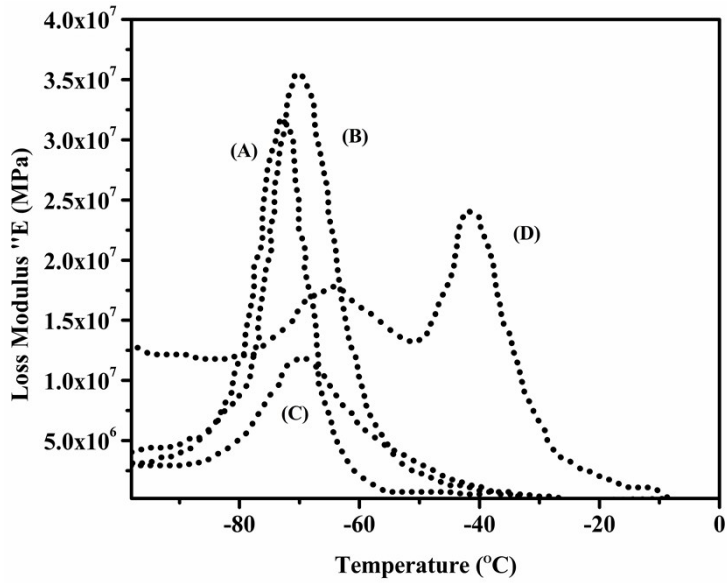


Figure 10. Variation of loss modulus with temperature for (A) 0 % Acyl-GAP, (B) 10 %, (C) 30 % (D) 50 %, (E) 70 % Acyl-GAP in NCO-*f*MWCNTs/HTPB: Alkyne-*f*MWCNTs/Acyl-GAP EIPNs.